Flame Speed and Self-Similar Propagation of Expanding Turbulent Premixed Flames

Swetaprovo Chaudhuri, Fujia Wu, Delin Zhu, and Chung K. Law*

Department of Mechanical and Aerospace Engineering, Princeton University, Princeton, New Jersey 08544-5263, USA

(Received 26 August 2011; published 27 January 2012)

In this Letter we present turbulent flame speeds and their scaling from experimental measurements on constant-pressure, unity Lewis number expanding turbulent flames, propagating in nearly homogeneous isotropic turbulence in a dual-chamber, fan-stirred vessel. It is found that the normalized turbulent flame speed as a function of the average radius scales as a turbulent Reynolds number to the one-half power, where the average radius is the length scale and the thermal diffusivity is the transport property, thus showing self-similar propagation. Utilizing this dependence it is found that the turbulent flame speeds from the present expanding flames and those from the Bunsen geometry in the literature can be unified by a turbulent Reynolds number based on flame length scales using recent theoretical results obtained by spectral closure of the transformed G equation.

DOI: 10.1103/PhysRevLett.108.044503 PACS numbers: 47.70.Pq, 47.27.Gs

The turbulent flame speed is a topic of wide interest in combustion and turbulence research as evidenced by the large volume of analytical [1–8], experimental [9–15], computational [16,17] and review literature [18–22] that has emerged in the past few decades. Its practical relevance can be readily appreciated by recognizing that, being a measure of flame surface density, it can be correlated to the volumetric heat release rate in a turbulent reacting flow. The problem is of considerable fundamental complexity, which is further compounded by the disagreement between theories as well as the high degree of scatter of the experimental turbulent flame speeds and their sensitivity on the geometry and type of the burner used in the investigation [19]—a major hindrance that has prevented its utilization as a meaningful physical quantity for predictions and for validating simulations of turbulent reacting flows.

Fundamentally, under the long-held assumption that the turbulent flame speed is a meaningful physical quantity, there is the interest to seek a unified scaling description, at least under some special flow conditions such as those in homogeneous isotropic turbulence. The most obvious choice of the flame parameters for such a scaling would be the planar laminar flame speed $S_L \sim (D\omega_b^0)^{0.5}$ and the corresponding laminar flame thickness $\delta_L \sim (D/\omega_b^0)^{0.5}$, assuming a local laminar flame structure exists, where D and ω_b^0 are the characteristic thermal diffusivity and reaction rate respectively [23]. The problem of turbulent flame propagation can then be considered as a geometric one in which the effect of turbulence is to wrinkle the flame at a multitude of length scales without perturbing the inner flame structure. Such a problem was considered analytically in [24]. It was shown that for a premixed flame which is statistically planar and steady in homogeneous isotropic turbulence given by $G(x, y, z, t) = G_0$ [3], the turbulent flame speed normalized by the corresponding laminar flame speed for large turbulent Reynolds number (Re_T) is given to the leading order by

$$S_T/S_L \sim \langle\sqrt{1 + \nabla g \cdot \nabla g}\rangle \sim \left[1 + \int_0^\infty k^2\Gamma(k)dk\right]^{1/2} \sim [(u_{\mathrm{rms}}/S_L)(\lambda_I/\delta_L)]^{1/2}. \quad (1)$$

Here, g defined as $g(x, y, z, t) = G_N - z$, is the fluctuating z distance of each of $G(x, y, z, t) = G_N$ interfaces from its corresponding mean position predefined as $z = G_N$. G_N is the level set value of the Nth interface, k is the wave number, and $\Gamma(k)$ is the g^2 spectrum obtained from the spectral closure of the autocorrelation equation of g [25], u_{rms} the root mean square of velocity fluctuations and λ_I the velocity integral length scale which was assumed to be the flame hydrodynamic length scale. This approximation was shown to be valid when $\partial g/\partial x_i$ follows Gaussian distribution or $(\partial g/\partial x_i)(\partial g/\partial x_i)$ follows log-normal distribution as is expected for scalar gradients in homogeneous isotropic turbulence.

In this Letter we present experimental turbulent flame speed data measured in constant-pressure expanding flames, propagating in nearly homogeneous isotropic turbulence. Utilizing the self-similar property of turbulent flame speeds evolving from the theory and experimental data presented, we shall show in due course that the normalized turbulent flame speeds measured from the present spherically expanding flames, as well as those from literature data on Bunsen flames, can be scaled by a single parameter: a turbulent Reynolds number based on the geometric and transport properties of the flame. A configurationally independent description of turbulent flame propagation in near homogeneous isotropic turbulence is thus proposed.

Experiments.—The experiments were conducted in a nearly constant-pressure apparatus that has been extensively employed in the study of laminar flames [26]. Briefly, the apparatus consists of an inner chamber situated within an outer chamber of much larger volume. The inner chamber is filled with the test combustible gas while the

outer chamber is filled with an inert gas of the same density. The two chambers can be opened to each other at the instant of spark ignition by rotating a sleeve that otherwise covers a matrix of holes connecting the two chambers, and the propagating flame is automatically quenched upon contacting the inert gas in the outer chamber. The flame propagation event is therefore basically isobaric because of the small volume of the inner chamber, hence preventing any perturbation by global pressure rise on the local flame structure. Another advantage of the design is that experiments can be conducted under high initial pressures, up to 60 bars as in the studies of Refs. [26,27], while preserving the integrity of the optical windows.

In the present investigation turbulence is generated by four orthogonally positioned fans as in [9] which continuously run during the entire flame propagation event, with the resulting cold flow field characterized by high-speed particle image velocimetry (HS-PIV). It was found that the root-mean-square velocity $u_{\rm rms}$ was a factor of 2 larger than the unavoidable radially inward mean flow $\langle U_r \rangle$ in the PIV measurement plane. However, $\langle U_r \rangle \leq 25\%$ of the mean flame propagation rate for all cases studied. It was ensured that the statistic $\langle u_x u_y \rangle \sim 0$, one of the necessary conditions for the turbulence being isotropic. Detailed flowfield statistics and quantification of near-isotropy are presented in the Supplemental Materials [28] available online. The experiments were conducted at pressures of 1, 2, 3 and 5 bars and with $u_{\rm rms}$ ranging from 1.34 to 6 m/s. The domain of experimentation was chosen to be $0.21 \leq \langle R \rangle / R_{\rm chamber} \leq 0.38$, identified from laminar flame speed experiments to avoid ignition and wall effects at the initial and final stages of flame propagation, respectively [29]. Additional experiments were also conducted at different ignition energies to ensure that the observed flame propagation features are not artifacts of spark ignition.

Results.—Fig. 1 shows a set of Schlieren images of methane−air turbulent premixed flames at an equivalence ratio of $\phi = 0.9$, with different $u_{\rm rms}$ and pressures, and at nearly the same $\langle R \rangle$ realized at different instants of their propagation. These images, obtained with a Phantom V7.3 high-speed camera at 8510 fps, show that with increasing $u_{\rm rms}$, the flame propagates faster on average, which is a well known feature, and slightly finer scale structures emerge due to the reduction of the Kolmogorov length scale as the velocity integral length scale ($\lambda_I \sim 4$ mm) is fixed. Furthermore, with increasing pressure, the flame also propagates faster, and the flame overall appears very

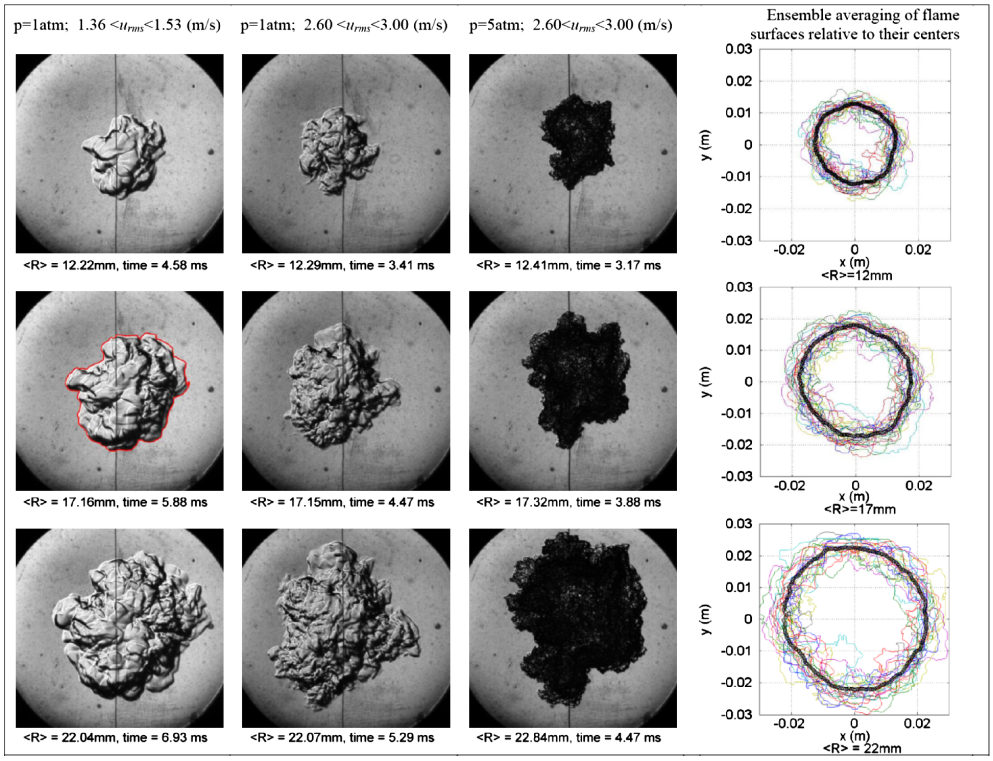

FIG. 1 (color online). High-speed Schlieren imaging at different $u_{\rm rms}$ and pressure, but at nearly same $\langle R \rangle$ showing the emergence of fine scale structures and associated increase in average propagation rate. The $u_{\rm rms}$ range specified above is the range experienced by the flame due to change in the largest length scale of the flame itself. Within the range 1–5 atm, $S_L^u \sim p^{-0.38}$, and $\delta_L \sim p^{-0.69}$ [38,39] resulting in $d\langle R \rangle / dt \sim p^{0.16}$. The fourth column shows instantaneous realizations of the flame fronts (thin colored lines) for same $\langle R \rangle$ values, at all conditions of $u_{\rm rms}$ and pressure where turbulent flame speeds are reported in this Letter. The thick black line shows a curve obtained by ensemble averaging over all the instantaneous flame fronts, the velocity integral length scale remaining constant.

different due to the emergence of very small scale structures. These fine structures indicate reduction of the thickness of the laminar flamelets with increasing pressure, which also allows flame surface wrinkling at progressively smaller scales. It is recognized that all these observations are not affected by any intrinsic flame instability as it was demonstrated by laminar flame propagation experiments that over the pressure range studied, essentially no Darrieus-Landau instability develops. Furthermore, since the mixture composition was selected such that its effective Lewis number (Le) is close to unity, onset of diffusive-thermal instability is suppressed and the effect of mean curvature on the mean propagation rate due to statistical sphericity of the flame should be negligible. In the data reduction, $\langle R \rangle$ is defined as $\langle R \rangle = \sqrt{A/\pi}$, where A is the area enclosed by the flame edge tracked from the high-speed Schlieren imaging using fully automated image processing Matlab routines utilizing Canny edge detection [30], representatively shown in the 2nd row, 1st column of Fig. 1. Even though the flames in Fig. 1 do not appear to be symmetric for individual realizations, ensemble averaging at the same $\langle R \rangle$ clearly produces near perfect symmetry, as shown in 4th column of Fig. 1.

To correlate the measured turbulent flame speed with the imposed turbulence parameters, Eq. (1) provides insight for self-similar propagation if λ_I is replaced with the relevant largest flame length scale, i.e., hydrodynamic length scale of flame surface fluctuations which should be a linear function of $2\pi\langle R \rangle$ or simply $\langle R \rangle$ itself. Consequently, in Fig. 2 we plot $d\langle R \rangle/dt$, derived from the experimentally obtained $\langle R \rangle$, normalized by the laminar flame speed with respect to the burned gas (S_L^b), as a function of $[(u_{\rm rms}/S_L)(\langle R \rangle/\delta_L)]$, i.e., the RHS of Eqn. (1) with the integral length scale being replaced by $\langle R \rangle$. The superscript b, as in S_L^b implies flame properties with respect to burned gas, whereas absence of a superscript implies flame properties with respect to unburned gas. Since the thermal diffusivity $D \sim S_L \delta_L$, the term $[(u_{\rm rms}/S_L)(\langle R \rangle/\delta_L)] = {\rm Re}_{T,\langle R \rangle}$ represents a turbulent Reynolds number with $\langle R \rangle$ being the length scale and the thermal diffusivity replacing the kinematic viscosity. It is then observed from Fig. 2 that all the data from different conditions of turbulence intensity and pressure, and at each instant of the propagation event, collapse reasonably well on a ${\rm Re}_{T,\langle R \rangle}^{\alpha}$ curve, with the exponent $\alpha = 0.54$ obtained by nonlinear least-square fitting over the entire relevant data set. This result therefore substantiates the possible validity of the 1/2-power scaling, as suggested by the theory of [24]. More importantly, it suggests that expanding turbulent flame propagation is self-similar, at least in the domain of interrogation, as evident from the relationship

$$(S_L^b)^{-1} d\langle R \rangle/dt = O(1)[(u_{\rm rms}/S_L)(\langle R \rangle/\delta_L)]^{1/2}. \quad (2)$$

The 1/2 power of Eq. (2) also indicates that the turbulent flame is accelerating. This is due to the fact that as the flame expands during propagation, its smallest wave number decreases resulting in a continuous increase in the integral of the $k^2\Gamma$ spectrum, as shown in Fig. 3.

It is important to note that the mechanism of flame acceleration proposed here is distinctly different than that proposed in [9], in which the flame acceleration is attributed to the increase of $u_{\rm rms}(\langle R \rangle)$ as experienced by the flame. We have experimentally found that the θ-averaged $u_{\rm rms}(\langle R \rangle) \sim \langle R \rangle^{0.25}$, which shows a much weaker dependence on $\langle R \rangle$

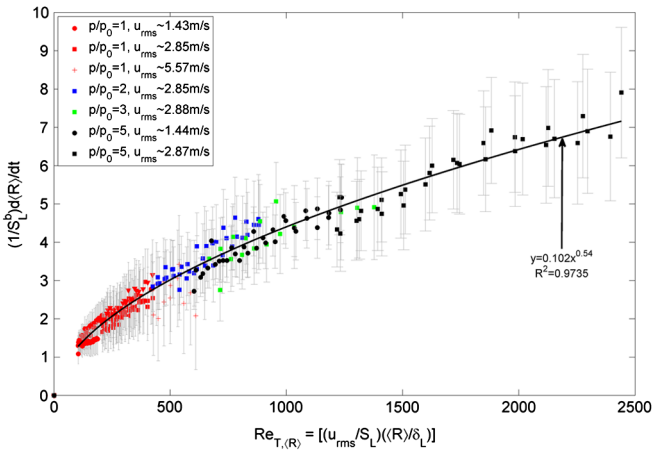

FIG. 2 (color online). Plot of flame propagation rate normalized by laminar burned flame speed with respect to turbulent Re with average radius as length scale and thermal diffusivity as transport property. Not included in the fitting is the $p/p_0 = 1$, $u_{\rm rms} \sim$ 5.57 m/s case as the Schlieren images show widespread local extinction in such flames and evident from their lower propagation rates. $u_{\rm rms}$ appearing in the abscissa is the $u_{\rm rms}(\langle R \rangle)$, obtained by integrating over all θ. $u_{\rm rms} \sim$ denotes the average $u_{\rm rms}$ experienced by the flames during the propagation event. The error bars indicate the error that could be caused by the mean flow.

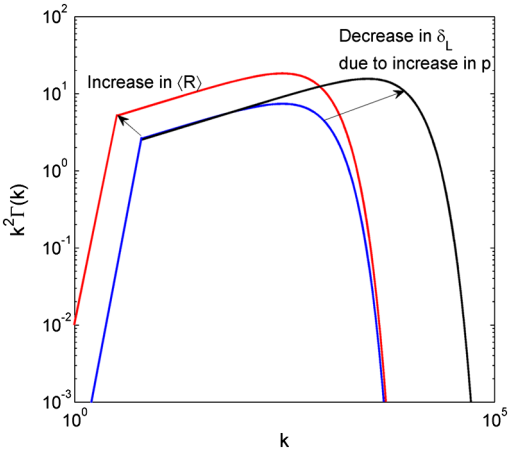

FIG. 3 (color online). Schematic of flame surface dissipation spectrum showing the effect of increase of the largest flame length scale: $\langle R \rangle$; decrease of the smallest length scale, i.e. δ_L, both causing increase in the area under the spectrum and thus increased turbulent flame speed ratio, specifically acceleration for an expanding flame.

than the near-linear scaling required to explain Eq. (2) and for collapsing all the data on a single curve as in Fig. 2. Theoretically, it can also be shown [24] that for large $\langle R\rangle$,

$$u_{\mathrm{rms}}(\langle R\rangle) \sim \left(\int_{k(\langle R\rangle)}^{\infty} \varepsilon^{2/3}k^{-5/3}\exp(-C(k\eta)^{4/3})dk\right)^{1/2} \sim \langle R\rangle^{1/3},$$

where ε is the mean kinetic energy dissipation rate and η is the Kolmogorov length scale. In comparison, the global average flame surface dissipation rate, i.e., the integral in Eq. (1), is given by [24],

$$\int_{k(\langle R\rangle)}^{\infty} k^2\Gamma(k)dk \sim \langle R\rangle;$$

where

$$\Gamma(k) = Bk^{-5/3}\exp\left(-\frac{3}{4}(2\pi)^{4/3}c_2\mathrm{Mk}\left(\frac{u_{\mathrm{rms}}}{S_L}\frac{\lambda_I}{\delta_L}\right)^{-1}(k/k_I)^{4/3}\right)$$

and Mk is the Markstein number. Thus, the turbulent flame speed can be effectively increased by stretching and raising the $k^2\Gamma$ spectrum, as shown in Fig. 3, towards higher or lower wave numbers by change of the smallest or largest flame length scales, respectively. This mechanism is believed to be of significance in explaining the acceleration of such expanding flames, which by its definition implies decrease of its smallest wave number. Furthermore, increasing pressure results in stretching the spectrum on the side of the higher wave number. The acceleration eventually ceases when the flame length scale $\langle R\rangle$ approaches the flow hydrodynamic length scale, at which the growth of the $k^2\Gamma$ spectrum is terminated.

Gas expansion effects and unification of turbulent flame speeds.—It is important to recognize that $d\langle R\rangle/dt \neq S_T^b$ due to gas expansion effects. An expanding turbulent flame with zero mean flow necessitates zero mean burned gas velocity boundary condition. This is satisfied by a radially outward gas expansion flow induced ahead of the flame given by $V_0 \sim (\Theta - 1)S_T$, where $\Theta = \rho_u/\rho_b$. According to measurements by Bradley *et al.* [31], $\langle R\rangle$ obtained by Schlieren imaging corresponds to the progress variable, $\langle c\rangle \sim 0.05 - 0.1$. This is reasonable as the Schlieren image, being a projection, contains interference of large-scale flame structures from planes other than the diametrical plane resulting in small but systematic overestimation of $\langle R\rangle$. Assuming that the location $\langle R\rangle$ lies predominantly in the unburned gas and free from density fluctuations, it can be shown that

$$\begin{aligned}\langle\rho_0\rangle 4\pi r_0^2(-S_{T,0}) &= \langle\rho_1\rangle 4\pi r_1^2(-S_{T,1}^b)\\ &= \langle\rho_{0.5}\rangle 4\pi r_{0.5}^2(-S_{T,0.5})\\ &\Rightarrow \langle\rho_0\rangle 4\pi r_0^2\mathbf{n}\cdot(\langle\mathbf{V_0}\rangle - d\langle\mathbf{R}\rangle/dt)\\ &= \langle\rho_1\rangle 4\pi r_1^2(-S_{T,1}^b)\\ &\Rightarrow d\langle R\rangle/dt = \Theta S_{T,0} = (r_1^2/r_0^2)S_{T,1}^b, \quad (3)\end{aligned}$$

where the numerical subscript denotes the $\langle c\rangle$ value.

It has been verified by measuring the Schlieren radius at each θ that the flame brush thickness $\delta_T \sim \langle R\rangle/2$, which implies that $S_{T,1}^b = 4(d\langle R\rangle/dt)$. Similarly, simple algebra yields

$$\begin{aligned}S_{T,0.5}/S_L &= (2\Theta/(\Theta+1))(r_0^2/r_{0.5}^2)(S_L^b)^{-1}(d\langle R\rangle/dt)\\ &= (28/9)(S_L^b)^{-1}(d\langle R\rangle/dt),\end{aligned}$$

for $\Theta = 7$ and assuming $\langle\rho_{0.5}\rangle = (\langle\rho_0\rangle + \langle\rho_1\rangle)/2$, which can be considered to be the normalized turbulent flame speed as it is defined on the location of the mean flame front, $\langle c\rangle = 0.5$.

This result can then be compared with experimental turbulent flame speeds determined from other geometries such as the widely used Bunsen flame. Extensive data over large pressure and turbulence intensity ranges have been reported in Kobayashi *et al.* [14,15]. However the two papers present measurements of the turbulent flame speed at two different $\langle c\rangle$ locations, with the more recent paper [15] measuring at $\langle c\rangle = 0.1$ and the earlier one [14] at $\langle c\rangle = 0.5$. For $\langle c\rangle = 0.1$, the gas expansion velocity is negligible and the configuration is statistically steady, while at $\langle c\rangle = 0.5$ there are non-negligible gas expansion effects, resulting in turbulent flame speeds with identical scaling but different prefactors. According to Smallwood *et al.* [32] the correction factors for converting the turbulent flame speed at $\langle c\rangle = 0.1$ to that at $\langle c\rangle = 0.5$ should be $\sim$1.2 to 1.5 for Bunsen flames at 1 atm pressure condition. Consequently, we choose the correction factor to be the average of the two, 1.35. This prefactor should not depend on pressure as the flame brush is mainly controlled by large-scale eddies while pressure causes reduction in the flame thickness, which is a small scale effect. The data are shown in Fig. 4 along with those from the present experiments as S_T/S_L versus $(\mathrm{Re}_{\lambda_{H,f}})^{1/2}$, i.e., a turbulent Reynolds number with the flame hydrodynamic length scale and flame transport properties. It is seen that the two data sets collapse quite well, hence suggesting the possibility of a unified turbulent flame speed correlation when it is appropriately scaled and corrected for gas expansion effects.

Remarks.—The major contributions and implications of this work are discussed in details in the Supplemental Material [28]. We further note that the self-similar propagation given by Eq. (2) may also imply a fractal structure, i.e., hierarchical clustering [33], as first proposed and discussed for hydrodynamically unstable expanding laminar flames without external forced turbulence [34,35] in which the flamefront wrinkling is due to the Darrieus-Landau instability. Furthermore, the fact that the turbulent flame undergoes acceleration would imply compression of the expanding gases ahead of the flame for suitably large accelerations [36]. This process, as well as high-intensity turbulence [37], could be possible mechanisms leading to the phenomenon of deflagration-to-detonation transition (DDT) in turbulent flow fields. Resolution of issues of such nature merits further study.

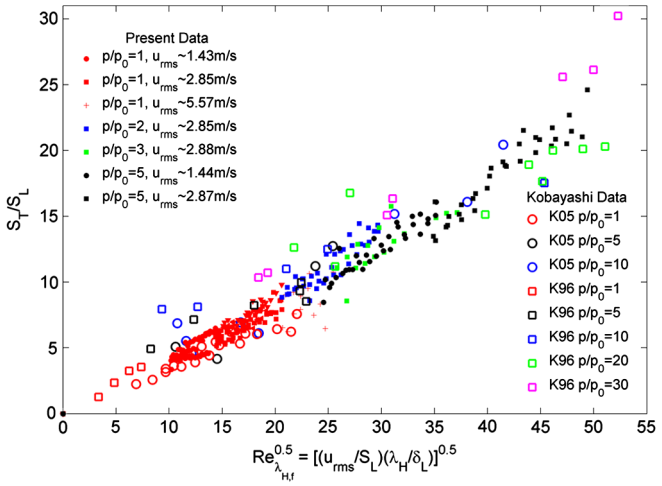

FIG. 4 (color online). Unifying turbulent flame speed from expanding flames (data from Fig. 2) and that from Kobayashi's experiments [14,15] by a turbulent Reynolds number to the 1/2-power scaling. The length scale is the instantaneous average flame radius in case of spherical flames and burner diameter for Bunsen flames. Kinematic viscosity is replaced by thermal diffusivity. The ordinate is $S_{T,0.5}/S_L$, chosen to appropriately represent the normalized turbulent flame speed.

This work was supported by the Combustion Energy Frontier Research Center, an Energy Frontier Research Center funded by the U. S. Department of Energy, Office of Basic Energy Sciences under Grant No. DE-SC0001198 and by the Air Force Office of Scientific Research.

*Corresponding author.
cklaw@princeton.edu

[1] P. Clavin and F. A. Williams, J. Fluid Mech. **90**, 589 (1979).
[2] V. Yakhot, Combust. Sci. Technol. **60**, 191 (1988).
[3] A. R. Kerstein, W. T. Ashurst, and F. A. Williams, Phys. Rev. A **37**, 2728 (1988).
[4] A. R. Kerstein and W. T. Ashurst, Phys. Rev. Lett. **68**, 934 (1992).
[5] A. Pocheau, Phys. Rev. E **49**, 1109 (1994).
[6] B. Denet, Phys. Rev. E **55**, 6911 (1997).
[7] N. Peters, J. Fluid Mech. **384**, 107 (1999).
[8] H. Kolla, N. Rogerson, and N. Swaminathan, Combust. Sci. Technol. **182**, 284 (2010).
[9] R. G. Abdel-Gayed, D. Bradley, and M. Lawes, Proc. R. Soc. A **414**, 389 (1987).
[10] D. Bradley, C. G. W. Sheppard, R. Woolley, D. A. Greenhalgh, and R. D. Lockett, Combust. Flame **122**, 195 (2000).
[11] D. Bradley, M. Lawes, and M. S. Mansour, Combust. Flame **158**, 123 (2011).
[12] S. A. Filatyev, J. F. Driscoll, C. D. Carter, and J. M. Donbar, Combust. Flame **141**, 1 (2005).
[13] S. Kwon, M. S. Wu, J. F. Driscoll, and G. M. Faeth, Combust. Flame **88**, 221 (1992).
[14] H. Kobayashi, T. Tamura, K. Maruta, and T. Niioka, Proc. Comb. Inst. **26**, 389 (1996).
[15] H. Kobayashi, K. Seyama, H. Hagiwara, and Y. Ogami, Proc. Comb. Inst. **30**, 827 (2005).
[16] J. B. Bell *et al.*, Proc. Natl. Acad. Sci. U.S.A. **102**, 10 006 (2005).
[17] Y. Shim, S. Tanaka, M. Tanahashi, and T. Miyauchi, Proc. Comb. Inst. **33**, 1455 (2010).
[18] N. Peters, *Turbulent Combustion* (Cambridge University Press, NY, 2000).
[19] J. F. Driscoll, Prog. Energy Combust. Sci. **34**, 91 (2008).
[20] A. N. Lipatnikov and J. Chomiak, Prog. Energy Combust. Sci. **36**, **1**, 1 (2010).
[21] A. N. Lipatnikov and J. Chomiak, Prog. Energy Combust. Sci. **28**, **1**, 1 (2002).
[22] S. B. Pope, Annu. Rev. Fluid Mech. **19**, 237 (1987).
[23] C. K. Law, *Combustion Physics* (Cambridge University Press, NY, 2006).
[24] S. Chaudhuri, V. Akkerman, and C. K. Law, Phys. Rev. E **84**, 026322 (2011).
[25] N. Peters, J. Fluid Mech. **242**, 611 (1992).
[26] S. D. Tse, D. L. Zhu, and C. K. Law, Rev. Sci. Instrum. **75**, 233 (2004).
[27] G. Rozenchan, D. L. Zhu, and C. K. Law, Proc. Comb. Inst. **29**, 1461 (2002).
[28] See Supplemental Material at http://link.aps.org/supplemental/10.1103/PhysRevLett.108.044503 for details.
[29] A. P. Kelley, G. Jomaas, and C. K. Law, Combust. Flame **156**, 1844 (2009).
[30] J. Canny, IEEE Trans. Pattern Anal. Mach. Intell. **PAMI-8**, 679 (1986).
[31] D. Bradley, M. Lawes, and M. S. Mansour, Combust. Flame **158**, 123 (2011).
[32] G. J. Smallwood, O. L. Gulder, D. R. Snelling, B. M. Deschamps, and I. Gokalp, Combust. Flame **101**, 461 (1995).
[33] U. Frisch, *Turbulence* (Cambridge University Press, Cambridge, England, 2000).
[34] Yu. A. Gostintsev, A. G. Istratov, Yu. V. Shulenin, Combustion, Explosion and Shock Waves (English Translation)(1965-) / Combust, Explos Shock Waves **24**, 563 (1989).
[35] Yu. A. Gostintsev, A. G. Istratov, and V. E. Fortov, Doklady Akademii Nauk **353**, 55 (1997).
[36] V. Akkerman, C. K. Law, and V. Bychkov, Phys. Rev. E **83**, 026305 (2011).
[37] A. Y. Poludnenko, T. A. Gardiner, and E. S. Oran, Phys. Rev. Lett. **107**, 054501 (2011).
[38] R. J. Kee *et al.*, CHEMKIN Collection, Release 3.6, 2000.
[39] H. Wang *et al.*, USC Mech Version II. *High-Temperature Combustion Reaction Model of H2/CO/C1C4 Compounds, May 2007*, http://ignis.usc.edu/USC_Mech_II.htm.